Van Paepegem, W. and Degrieck, J. (2001). Experimental Setup for and Numerical Modelling of Bending Fatigue Experiments on Plain Woven Glass/epoxy Composites. *Composite Structures*, 51(1), 1-8.

Experimental setup for and numerical modelling of bending fatigue experiments on plain woven glass/epoxy composites

W. Van Paepegem[a*] and J. Degrieck[b]

[a] Research Assistant of the Fund for Scientific Research – Flanders (F.W.O.), Dpt. of Mechanical Construction and Production, Sint-Pietersnieuwstraat 41, 9000 Gent, Belgium
[b] Professor, Dpt. of Mechanical Construction and Production, Sint-Pietersnieuwstraat 41, 9000 Gent, Belgium

Abstract

In general fatigue of fibre-reinforced composite materials is a quite complex phenomenon, and a large research effort is being spent on it today. Due to deficiencies in the current life prediction methodologies for these materials, composite structures are often overdesigned: large factors of safety are adopted and extensive prototype-testing is required to allow for an acceptable life time prediction. This paper presents an investigation of the fatigue performance of plain woven glass/epoxy composite materials and of the numerical modelling of these composites' behaviour under fatigue.
First the experimental setup which has been developed for bending fatigue experiments, is discussed. The materials used are plain woven glass/epoxy specimens in two configurations: $[\#0^\circ]_8$ and $[\#45^\circ]_8$. Experiments show that these two specimen types, although being made of the same material, have a quite different damage behaviour and that the stiffness degradation follows a different path.
Next a numerical model is presented which allows one to describe the degradation behaviour of the composite specimen during its fatigue life. This model has been implemented in a mathematical software package (Mathcad™) and proves to be a useful tool to study the fatigue degradation behaviour of composite materials.

Keywords: fatigue, composites, bending experiments, damage model, residual stiffness

1 Introduction

Fibre-reinforced composite materials are finding increasing application in aerospace structures, naval industry and other high-tech designs, because of their high specific stiffness and strength. Although the fatigue behaviour of fibre-reinforced composites has been studied for a long time, it is still not possible to make adequate predictions about the fatigue life and degradation of stiffness and strength without extensive 'ad hoc' investigation.
Research on fatigue of composite materials is conducted by performing numerous fatigue experiments, whereby tension-tension fatigue and tension-compression fatigue are the most favourable ways of working, since damage is developing more or less equally in all layers of the composite specimen (Fuji et al. [1], Schulte et al. [2] and Hansen [2]). Bending fatigue experiments on the other hand have been reported by only a few authors (Ferry et al. [3], Herrington and Doucet [5] and Chen and Matthews [6]). Although fatigue experiments in tension and compression remain indispensable for accurately modelling the fatigue behaviour of composites, bending fatigue experiments yield a lot of useful information as well:

- stresses and strains can vary along the gauge length of the specimen. Damage is thus varying gradually along the specimen length, providing much more information from one experiment,
- the different behaviour and damage development of the specimen at the tension- and compression side can be monitored for any tension-compression ratio,

* Author to whom correspondence should be addressed (E-mail: Wim.VanPaepegem@rug.ac.be).

- and permanent deformations of the composite specimen can be easily measured.

Although stresses nor strains are constant along the length of the specimen (only a constant displacement is imposed at the lower end of the specimen (see infra)), the geometry and loading conditions are very simple, such that numerical validation and geometrical modelling are relatively straightforward.

2 Material and testing procedures

The material used in this study is a plain woven glass/epoxy composite. The plain woven glass fabric was stacked in eight layers, with two different stacking sequences. With the first type, the warp direction of all eight layers was aligned with the loading direction (denoted as $[\#0^\circ]_8$, where '0°' means that the warp direction of each of the eight layers has been aligned with the loading direction and where the symbol '#' refers to the fabric reinforcement type). With the second stacking sequence, the angle between the warp direction of all layers and the loading direction was 45º (denoted as $[\#45^\circ]_8$). All composite specimens were manufactured using the resin-transfer-moulding technique. After curing they had a thickness of 2.72 mm. The samples were cut to dimensions of 145 mm long by 30 mm wide on a water-cooled diamond saw.

The in-plane elastic properties of the composite laminates were determined using dynamic modal analyis (Sol et al. [7]). They are listed in Table 1.

Table 1 Measured in-plane elastic properties of the composite laminates

E_{11} (GPa)	24.57
E_{22} (GPa)	23.94
ν_{12} (-)	0.153
G_{12} (GPa)	4.83

These values compare very well with a micromechanical analysis, where the properties of the E-glass fibre and the epoxy matrix are filled in separately. Each woven layer is modelled as two unidirectional layers, stacked in a [0º/90º] sequence. With the fibre volume fraction ν_f being 0.48, the estimated homogenized properties are listed in Table 2.

Table 2 Estimated in-plane elastic properties of the composite laminates

E_{11} (GPa)	23.51
E_{22} (GPa)	23.51
ν_{12} (-)	0.143
G_{12} (GPa)	3.95

3 Experimental setup for bending fatigue

The experimental setup was developed specially for flexural fatigue tests on cantilever beam specimens and is shown in Figure 1. Although more sophisticated commercial servohydraulic testing machines are capable of performing the same fatigue experiments, the maintenance and service costs are very high, compared to the costs of use of this testing machine.

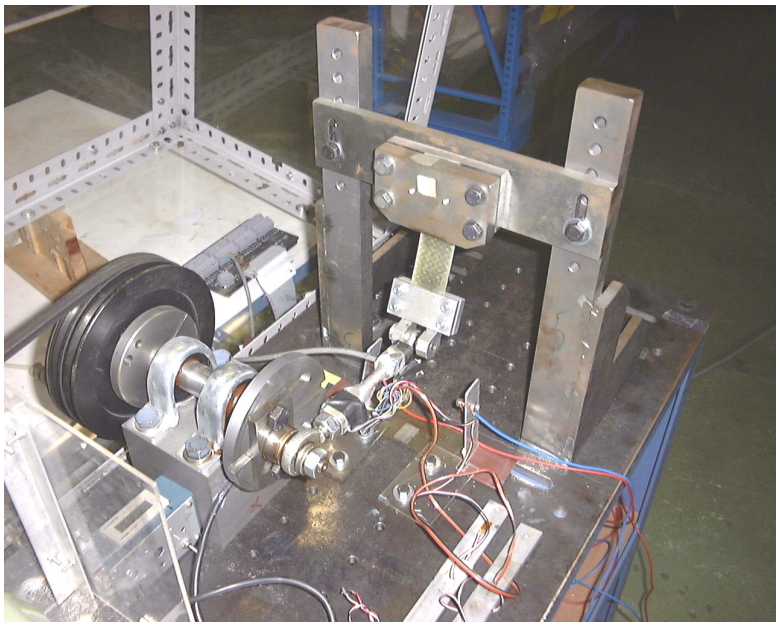

Figure 1 Experimental setup for bending fatigue experiments.

The outcoming shaft of the motor has a rotational speed of 185 rpm. The power is transmitted by a V-belt to a second shaft, which provides a fatigue testing frequency of 2.23 Hz. The influence of frequency can be assumed to be small in this range of values (Manger et al. [8]). The power transmission through a V-belt ensures that the earthing of the motor and the earthing of the measurement system are electrically isolated.

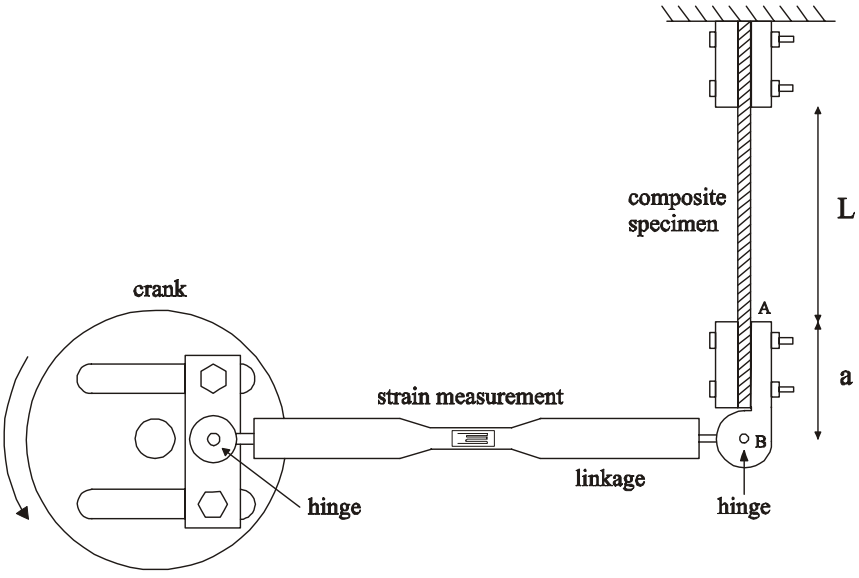

Figure 2 Schematic drawing of the crank-linkage mechanism.

The second shaft bears a crank-linkage mechanism, which is shown in Figure 2. This mechanism imposes an alternating displacement on the hinge (point B) that connects the linkage with the lower clamp of the composite specimen. At the upper end the specimen is clamped. Hence the samples are loaded as a composite cantilever beam. The amplitude of the imposed displacement is a controllable parameter and the adjustable crank allows to choose

between single-faced and double-faced bending, i.e. the deflection can vary from zero to the maximum deflection in one direction, respectively in two opposite directions.
A full Wheatstone bridge on the linkage is used to measure the force acting on the composite specimen. The selection of the strain gauges had to be done carefully, since the linkage is fatigued as well and internal energy dissipation leads to small temperature rises at the site of the active strain gauges, which are not compensated by the dummy strain gauges in the neighbourhood. Therefore two self-temperature compensated strain gauges are placed on the two opposite surfaces of the linkage and they measure both the longitudinal and transverse strains. In that way temperature effects, as well as small bending moments, are compensated.

4 Experimental results

As mentioned above, two stacking sequences were used: $[\#0^\circ]_8$ and $[\#45^\circ]_8$ specimens. The stacking sequence $[\#0^\circ]_8$ is schematically illustrated in Figure 3.

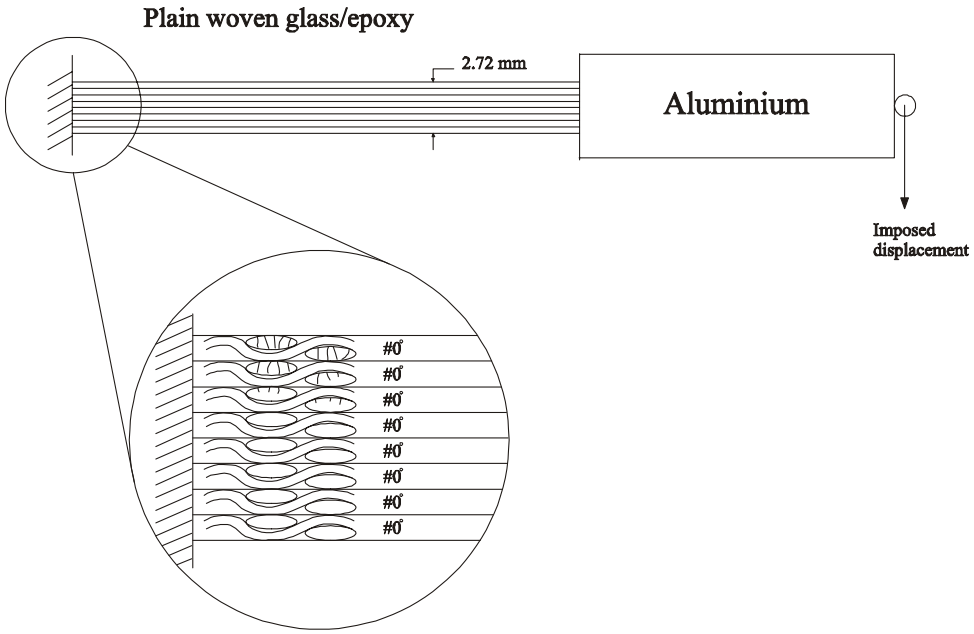

Figure 3 Definition of the $[\#0^\circ]_8$ stacking sequence for plain woven glass/epoxy specimens.

Fatigue experiments were performed with different values of the imposed displacement, as well as with single- and double-faced bending. To characterize each experiment, the 'displacement ratio' $R_d = \frac{u_{min}}{u_{max}}$ (analogous to the stress ratio R) is defined, whereby the minimum deflection is not necessarily zero. When the displacement u_{max} and the length L between the both clamps (Figure 2) are given too, all parameters of the fatigue experiment are determined.
Now some remarkable observations from the bending fatigue experiments are discussed.
When the maximum displacement u_{max} is the same for both specimens, the stiffness degradation path is quite different for $[\#0^\circ]_8$ and $[\#45^\circ]_8$ specimens. Figure 4 shows typical force-cycle histories for both stacking sequences. The abscis contains the number of cycles;

the ordinate axis shows the force (Newton), which is measured by the strain gauge bridge during the fatigue tests at constant bending displacement.

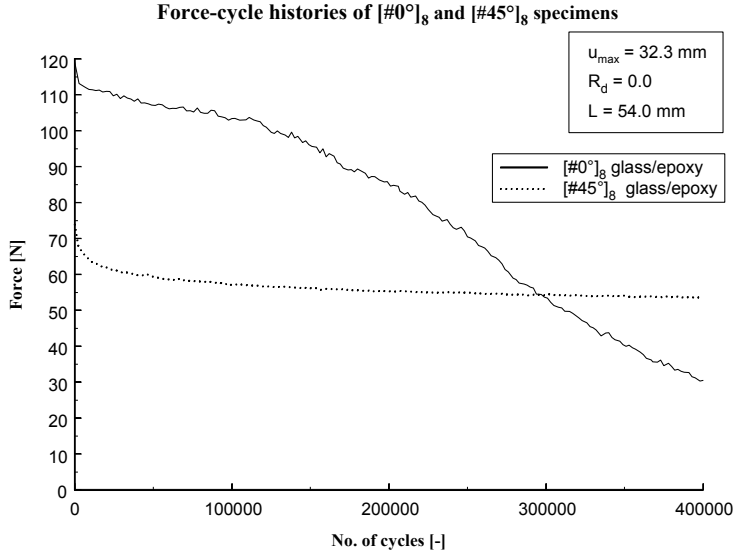

Figure 4 Bending fatigue performance of $[\#0°]_8$ and $[\#45°]_8$ specimens at constant bending displacement.

The $[\#0°]_8$ specimens degrade gradually and their stiffness is reduced significantly after 400,000 cycles. The initial force on the $[\#45°]_8$ specimens is smaller, because their stiffness is lower. However, after nearly 300,000 cycles, their remaining stiffness has become larger than that of the $[\#0°]_8$ specimens.
Not only the force-cycle histories are different for both specimen types; Figure 5 shows that their fatigue damage pattern differs as well.

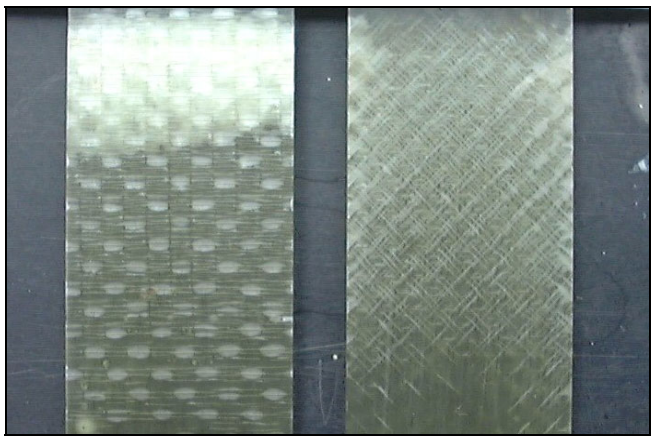

Figure 5 Degradation of a $[\#0°]_8$ (left) and a $[\#45°]_8$ (right) specimen.

In the $[\#0°]_8$ specimens, several fibres are broken at the clamped end of the specimen and a sort of 'hinge' is formed, while in the $[\#45°]_8$ specimens a more regular pattern is found. Further away from the fixation a regular pattern of transverse cracking in the weft tows at the fabric cross-over points is shown in the $[\#0°]_8$ specimens (see also zoomed-in drawing in Figure 3). This 'characteristic damage state' is very similar to the steady state matrix cracks in tension fatigue (Fujii et al. [1] and Manger et al. [8]).

With both types of specimens, the outermost layers which have been subjected to the largest tensile stresses, are severely damaged, while the outermost layers at the compression side show no observable sign of damage. This brings about an important result: due to the growth of damage and the degradation of the bending stiffness, there is a continuous redistribution of the stresses in the cross-section, especially near the fixation where damage growth is dominant. The position of the 'neutral fibre' (according to its definition in the classical beam theory) does not remain in the middle of the cross-section, but tends to move towards the compression side and transfers the load to that zone.
Further a considerable permanent deformation did remain after removing the grips from the $[\#45°]_8$ specimens, while this is not the case for the $[\#0°]_8$ specimens. Such deformations are difficult to observe when specimens are loaded in fatigue tension and/or compression because of the very small displacements, but are easy to measure in bending, because the displacements are much larger. The bending fatigue experiments thus show that a more generalized fatigue damage model should take into account the accumulation of permanent strain for certain stacking sequences.

Another interesting observation is that there exists a 'fatigue threshold stress' in bending. Figure 6 illustrates a typical experiment on a $[\#0°]_8$ specimen. The imposed displacement ranges from zero to a maximum value and the specimens always bends in the same direction (single-faced bending). First the composite specimen has been fatigued during 770,000 cycles with a small constant-amplitude displacement (u_{max} = 7.1 mm). The force, necessary to bend the composite specimen and measured by the Wheatstone bridge, is constant during these 770,000 cycles and equals approximately 20 N. Next a larger displacement (u_{max} = 29.5 mm) is imposed, which is held constant during 530,000 cycles more. Then indeed degradation is initiating and growing fast, until complete damage has occurred.

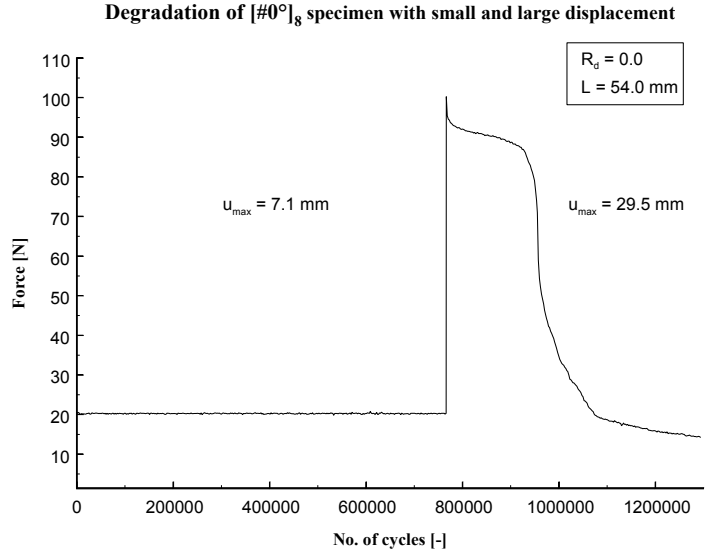

Figure 6 Degradation of a $[\#0°]_8$ specimen at a small and a large constant displacement.

Figure 4 and Figure 5 illustrate that the degradation of the $[\#45°]_8$ specimens is mainly due to matrix cracks and shows a very gradual path with a sharp initial stiffness reduction. Therefore in the next paragraph a damage accumulation model is proposed to describe the experimental observations through numerical simulations for the $[\#45°]_8$ specimens. The simulation for the

$[\#0°]_8$ specimens requires a more complex model, because several damage mechanisms are acting together (matrix cracks, fibre-matrix interface failure, fibre fracture).

5 Local damage model

In the opinion of the authors, fatigue models can be classified in three major categories:
- fatigue life models, which do not take into account the actual degradation mechanisms but use S-N curves (influence of stress amplitude on occurrence of final failure) or Goodman-type diagrams (influence of mean stress level) and introduce some sort of fatigue failure criterion,
- residual strength models, which describe the degradation of the initial static strength, equally without taking into account stiffness reduction,
- and finally damage accumulation models which use one or more damage variables related to measurable manifestations of damage (number of transverse matrix cracks, delamination size) or to the residual stiffness.

Although the fatigue behaviour of fibre-reinforced composites is fundamentally different from the behaviour exposed by metals, many models have been established which are based on the well-known S-N curves. This approach requires extensive experimental work and does not take into account the actual damage mechanisms, such as matrix cracks and fibre fracture.
With regard to residual strength models, measurement of strength during damage development in a material is not feasible, because it is a destructive method and only one measurement can be made for one specimen. Moreover it is very difficult to compare damage states between two specimens, because the scatter on the strength is large compared to the scatter on the stiffness. On the other hand stiffness can be measured frequently or even continuously during damage development and does not affect the damage development as such. Therefore stiffness is a potential non-destructive parameter which can be used to monitor the in-service fatigue damage in the composite specimen.
Further, in a fibre-reinforced composite the extent of the damage zones grows, while the damage-type in these zones can change (e.g. small matrix cracks leading to large size delaminations). The gradual deterioration of a fibre-reinforced composite – with a loss of stiffness in the damaged zones – leads to a redistribution of stress and a reduction of stress concentrations in a structural component. As a consequence an appraisal of the actual state or a prediction of the final state (when and where final failure is to be expected) requires the simulation to follow the complete path of successive damage states.
This is confirmed by the experiments which show that the normal stresses acting on the cross-sectional area of the clamped end, are redistributed during fatigue life and that the neutral fibre (according to the definition used in beam theory) is moving across the height of the specimen, because damage in the outermost layers at the tensile side is growing much faster than in the neighbouring zones.
Therefore numerical calculations at decisive stages in fatigue life, which take into account the stiffness degradation, are indispensable to make an estimate of the redistribution of the stresses over the structure. Here a unidirectional model for fatigue damage is proposed. One local damage variable D is associated with the longitudinal stiffness loss. The stresses and strains are then related by the commonly used equation:

$$\sigma = E_0.(1-D).\varepsilon \tag{1}$$

Strains are calculated with the equations of classical beam theory for a cantilever beam that is loaded with a force and a moment in the point A (see Figure 2).

The form for the fatigue evolution law is given by:

$$\frac{dD}{dN} = \begin{cases} \dfrac{A.(\Delta\sigma)^c}{(1-D)^b} & \text{in tension} \\ 0 & \text{in compression} \end{cases} \tag{2}$$

where:
- D : local damage variable
- N : number of cycles
- $\Delta\sigma$: amplitude of the applied cyclic loading
- A, b and c : three material constants

This damage law is similar to the one proposed by Sidoroff and Subagio [9], but uses the stress amplitude instead of the strain amplitude.
When the axial force is supposed to remain zero and when only a bending moment exists, the position of the neutral fibre y_0 at each moment of time is calculated as:

$$y_0 = \frac{\int_{-\frac{h}{2}}^{+\frac{h}{2}} [1-D(y)].y\, dy}{\int_{-\frac{h}{2}}^{+\frac{h}{2}} 1-D(y)\, dy} \tag{3}$$

where:
- y : thickness-coordinate, with y = 0 in the middle of the specimen's thickness
- h : total thickness of the specimen

The degraded bending stiffness EI becomes (with 'b' the specimen's width):

$$EI = b.E_0.\int_{-\frac{h}{2}}^{+\frac{h}{2}} [1-D(y)].y^2\, dy \tag{4}$$

The remaining equation is formed by using the principle of virtual work and where F is solved from this transcendental equation:

$$u_{max} = F.u_F + F.a.u_M + a.\sin(F.a.\alpha_M + F.\alpha_F) \tag{5}$$

where:
- F : force measured by the strain gauges and acting on the hinge (point B in Figure 2)
- a : length of the lower clamp (Figure 2)
- u_F and α_F : displacement, respectively rotation angle for a unit force F = 1 N in the point A (Figure 2)
- u_M and α_M : displacement, respectively rotation angle for a unit moment M = 1 Nm in the point A (Figure 2)

This numerical model can be easily implemented in a mathematical software package such as Mathcad™. The numerical integration formulas must be chosen such that the second degree polynomials are exactly integrated. This is the case for the Simpson's rule, which is a Newton-Cotes quadrature formula. Because the increase of the damage variable D during one cycle is so small, the integrations must be exact indeed, otherwise the relative error on the calculation of the bending stiffness EI may be larger than the increase of the damage variable itself. Therefore the conventional first-order trapezium method is not suited for this purpose.

Figure 7 shows the experimental and simulated results for the $[\#45°]_8$ specimen for which the force-cycle history was shown in Figure 4. The imposed displacement u_{max} is 32.3 mm, the displacement ratio R_d is zero and the length L (Figure 2) is 54.0 mm. The measured force initially equals 74.0 N, the total number of cycles in the experiment is 400,000 and the measured remaining force then equals 53.3 N. With regard to the simulation, the composite specimen is modelled with a mesh of 400 integration points and the calculation uses 40 integration steps. The values of the constants A, b and c (see equation (2)) are respectively: 10^{-18}, 0.45 and 6.5. The remaining force at 400,000 cycles is 51.7 N, which results in an error of only 3% after 400,000 cycles.
There is a very good agreement between the experimental data and the theoretical simulation, which proves that the proposed damage law is capable of simulating the kind of fatigue degradation behaviour that has been observed with $[\#45°]_8$ specimens.

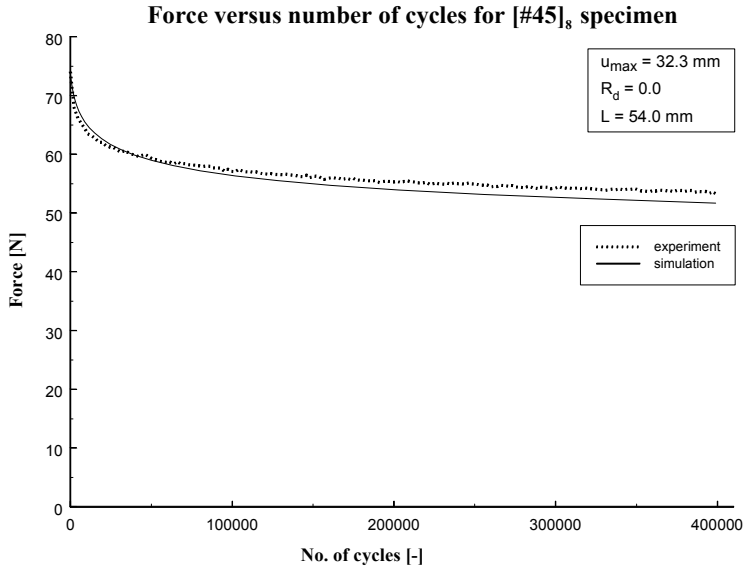

Figure 7 Degradation of the force versus the number of cycles for a $[\#45°]_8$ specimen.

Figure 8 shows the results from another experiment for a $[\#45°]_8$ specimen. Again the imposed displacement u_{max} is 32.3 mm, the displacement ratio R_d is zero and the length L is 54.0 mm. This specimen has a slightly lower modulus of elasticity, which results in a lower initial force of 65.3 N. After 399,000 cycles, the remaining force is 50.1 N.
For the simulation the values of the constants A, b and c remain the same (respectively: 10^{-18}, 0.45 and 6.5). The force after 399,000 cycles equals 48.2 N for the simulation, which results in an error of 3.8%.
The simulated results from this experiment can be used now for a more detailed discussion of the strain-, stress- and damage distributions in the composite specimen during fatigue life.

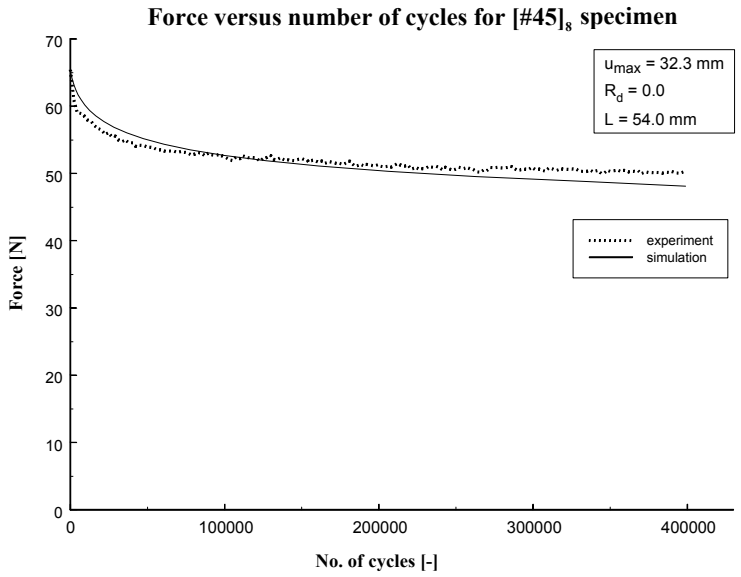

Figure 8 Degradation of the force versus the number of cycles for a $[\#45°]_8$ specimen.

Figure 9 shows the strain distribution over the cross-section near the clamped end at a few decisive stages in fatigue life. The ordinate axis represents the height y (mm) in the cross-section. As mentioned above the specimens have a thickness of 2.72 mm, so the coordinates of the integration points are in the range (-1.36 mm, +1.36 mm). At the first cycle, the tensile and compressive strain are equal and the strain is zero in the middle of the cross-section. When damage is growing, the neutral fibre is moving towards the compression side of the specimen.

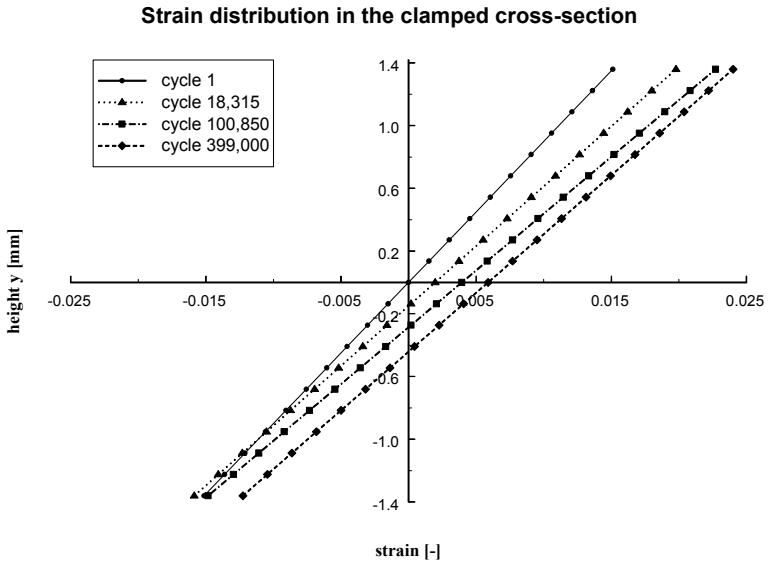

Figure 9 Strain distribution in the clamped cross-section.

The influence of damage can be observed even more clearly when the distribution of the stresses is calculated, as shown in Figure 10. At the first cycle, the stress distribution is linear and the normal stress is zero in the middle of the cross-section. When damage is initiating, the tensile stresses in the outermost layers are relaxed and load is transferred towards the inner layers. Because the damage law assumes that there is no damage growth at the compressive

side, the peak tensile stresses are moving towards the compression side and as a consequence the neutral fibre is moving down.

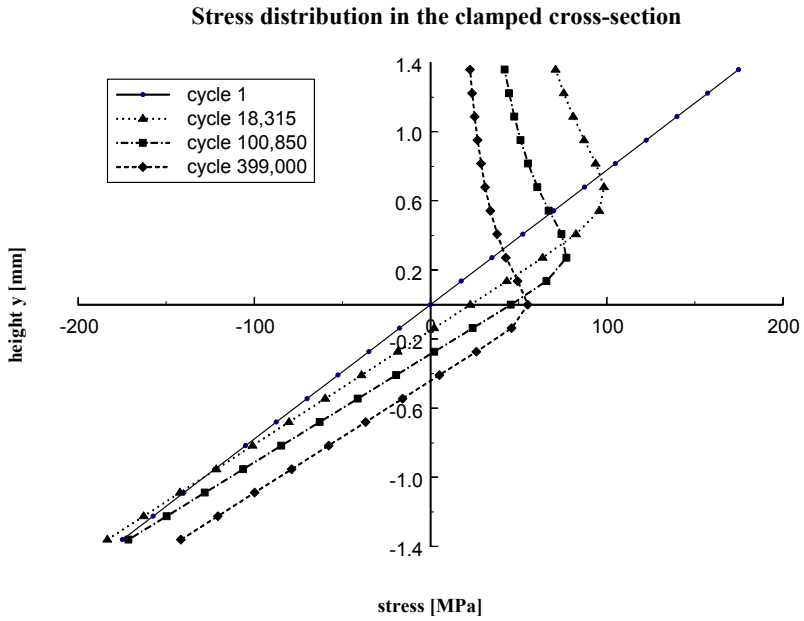

Figure 10 Stress distribution in the clamped cross-section.

Finally Figure 11 shows the damage growth in the integration points in the cross-section. The value of the damage variable D is lying between zero (no damage) and one (final failure of that integration point).
This damage distribution indeed reflects the experimental observations, where the outermost layers at the tension side are severely damaged ($D \approx 1$), while the compression side shows no observable damage.

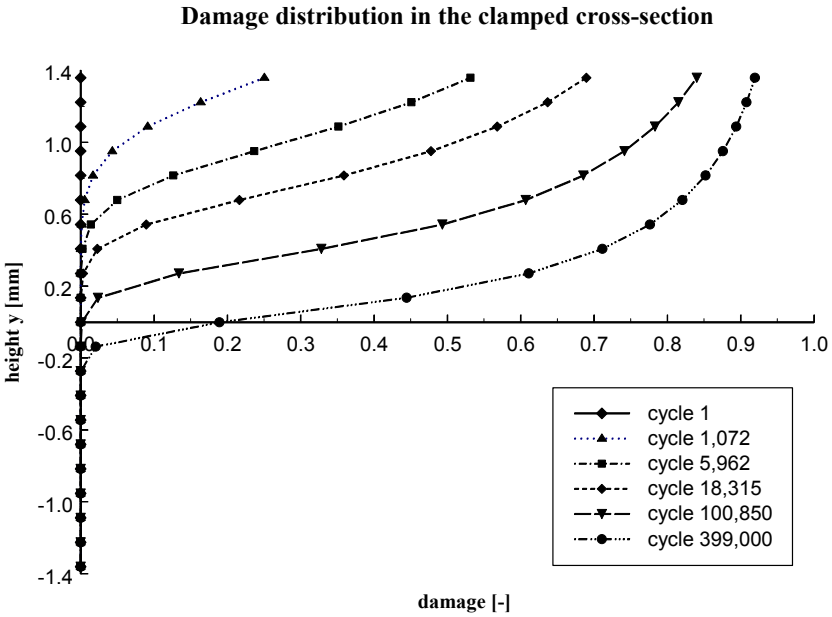

Figure 11 Damage distribution in the clamped cross-section.

Further investigation is required to incorporate some other experimental observations into the damage accumulation model, such as the accumulation of permanent strain in case of the $[\#45°]_8$ specimens and the existence of a 'fatigue threshold stress'. This will probably lead to a fatigue model, where damage initiation and propagation will be described by different terms in the damage evolution law. Next the fatigue damage behaviour of the $[\#0°]_8$ specimens will require a more complex damage accumulation model, because more than one damage mechanism is present: matrix cracking, fibre-matrix interface failures and fibre fracture.
However the discussed results prove that a damage accumulation model, related to the degradation of the stiffness properties, is capable of predicting a continuous redistribution of stresses across the structure, as can be observed in the experiments.

6 Conclusions

An experimental setup for bending fatigue experiments has been built. Results show that bending fatigue tests yield important additional information that cannot be recovered from the conventional tension fatigue tests.
A damage accumulation model has been proposed that allows to check the experimentally observed damage initiation and growth. The fatigue model can be easily implemented in a mathematical software package and shows good agreement for simulations of the degradation behaviour of $[\#45°]_8$ specimens.
The experiments indicate that stresses are continuously redistributed across the structure during fatigue life. As the damage accumulation model accounts for the degradation of the local stiffness properties, the stress redistribution can be theoretically simulated and the damage initiation and growth can be predicted.

Acknowledgements

The author W. Van Paepegem gratefully acknowledges his finance through a grant of the Fund for Scientific Research – Flanders (F.W.O.).
The authors also express their gratitude to Syncoglas for their support and technical collaboration.

References

1. Fujii, T., Amijima, S. and Okubo, K. (1993). Microscopic fatigue processes in a plain-weave glass-fibre composite. *Composites Science and Technology*, 49, 327-333.

2. Schulte, K., Reese, E. and Chou, T.-W. (1987). Fatigue behaviour and damage development in woven fabric and hybrid fabric composites. In : Matthews, F.L., Buskell, N.C.R., Hodgkinson, J.M. and Morton, J. (eds.). Sixth International Conference on Composite Materials (ICCM-VI) & Second European Conference on Composite Materials (ECCM-II) : Volume 4. Proceedings, 20-24 July 1987, London, UK, Elsevier, pp. 4.89-4.99.

3. Hansen, U. (1997). Damage development in woven fabric composites during tension-tension fatigue. In : Andersen, S.I., Brøndsted, P., Lilholt, H., Lystrup, Aa., Rheinländer, J.T., Sørensen, B.F. and Toftegaard, H. (eds.). Polymeric Composites - Expanding the Limits. Proceedings of the 18th Risø International Symposium on Materials Science, 1-5 September 1997, Roskilde, Denmark, Risø International Laboratory, pp. 345-351.

4. Ferry, L., Gabory, D., Sicot, N., Berard, J.Y., Perreux, D. and Varchon, D. (1997). Experimental study of glass-epoxy composite bars loaded in combined bending and torsion loads. Fatigue and characterisation of the damage growth. In : Degallaix, S., Bathias, C. and Fougères, R. (eds.). International Conference on fatigue of composites. Proceedings, 3-5 June 1997, Paris, France, La Société Française de Métallurgie et de Matériaux, pp. 266-273.

5. Herrington, P.D. and Doucet, A.B. (1992). Progression of bending fatigue damage around a discontinuity in glass/epoxy composites. *Journal of Composite Materials*, 26(14), 2045-2059.

6. Chen, A.S. and Matthews, F.L. (1993). Biaxial flexural fatigue of composite plates. In : Miravete, A. (ed.). ICCM/9 Composites : properties and applications. Volume VI. Proceedings of the Ninth International Conference on Composite Materials, 12-16 July 1993, Madrid, Spain, Woodhead Publishing Limited, pp. 899-906.

7. Sol, H., Hua, H., De Visscher J., Vantomme, J. and De Wilde, W.P. (1997). A mixed numerical/experimental technique for the nondestructive identification of the stiffness properties of fibre reinforced composite materials. *NDT&E International*, Vol. 30(2), pp. 85–91.

8. Manger, C.I.C., Ogin, S.L., Smith, P.A. and Greaves, R.P. (1997). Damage development in plain weave GFRP. In : Scott, M.L. (ed.). ICCM/11 Volume V : Textile composites and characterisation. Proceedings of the Eleventh International Conference on Composite Materials (ICCM/11), 14-18 July 1997, Gold Coast, Queensland, Australia, Woodhead Publishing Limited, pp. V.58-V.66.

9. Sidoroff, F. and Subagio, B. (1987). Fatigue damage modelling of composite materials from bending tests. In : Matthews, F.L., Buskell, N.C.R., Hodgkinson, J.M. and Morton, J. (eds.). Sixth International Conference on Composite Materials (ICCM-VI) & Second European Conference on Composite Materials (ECCM-II) : Volume 4. Proceedings, 20-24 July 1987, London, UK, Elsevier, pp. 4.32-4.39.